Oncogene (2008) 27, 3102–3110

www.nature.com/onc

ORIGINAL ARTICLE

The FLT3 inhibitor PKC412 exerts differential cell cycle effects on leukemic cells depending on the presence of FLT3 mutations

T Odgerel[1], J Kikuchi[1], T Wada[1], R Shimizu[1], K Futaki[1], Y Kano[2] and Y Furukawa[1]

[1]*Division of Stem Cell Regulation, Center for Molecular Medicine, Jichi Medical School, Tochigi, Japan and* [2]*Division of Hematology, Tochigi Cancer Center, Tochigi, Japan*

PKC412 is a staurosporine derivative that inhibits several protein kinases including FLT3, and is highly anticipated as a novel therapeutic agent for acute myeloblastic leukemia (AML) carrying FLT3 mutations. In this study, we show that PKC412 exerts differential cell cycle effects on AML cells depending on the presence of FLT3 mutations. PKC412 elicits massive apoptosis without markedly affecting cell cycle patterns in AML cell lines with FLT3 mutations (MV4-11 and MOLM13), whereas it induces G_2 arrest but not apoptosis in AML cell lines without FLT3 mutations (THP-1 and U937). In MV4-11 and MOLM13 cells, PKC412 inactivates Myt-1 and activates CDC25c, leading to the activation of CDC2. Activated CDC2 phosphorylates Bad at serine-128 and facilitates its translocation to the mitochondria, where Bad triggers apoptosis. In contrast, PKC412 inactivates CDC2 by inducing serine-216 phosphorylation and subsequent cytoplasmic sequestration of CDC25c in THP-1 and U937 cells. As a result, cells are arrested in the G_2 phase of the cell cycle, but do not undergo apoptosis because Bad is not activated. The FLT3 mutation-dependent differential cell cycle effect of PKC412 is considered an important factor when PKC412 is combined with cell cycle-specific anticancer drugs in the treatment of cancer and leukemia.
Oncogene (2008) **27**, 3102–3110; doi:10.1038/sj.onc.1210980; published online 10 December 2007

Keywords: FLT3 inhibitor; leukemia; cell cycle; CDC2; CDC25; Bad

Introduction

FMS-like tyrosine kinase-3 (FLT3) is a member of class III receptor tyrosine kinases, and is expressed on hematopoietic stem/progenitor cells. The binding of FLT3 ligand induces dimerization and autophosphorylation of FLT3, and subsequently activates multiple signal transduction pathways favoring cell survival and proliferation (Lyman *et al.*, 1993; Small *et al.*, 1994). FLT3 is also expressed in the majority of acute leukemias and is overexpressed in many cases (Gilliland and Griffin, 2002). In addition, its mutations are found in approximately 30% of patients with acute myeloblastic leukemia (AML), and accordingly, these are the second most common genetic alterations in AML. FLT3 mutations include internal tandem duplication of the juxtamembrane domain (FLT3-ITD) and point mutations in the activating loop, both of which result in ligand-independent activation of FLT3. The constitutive activation of FLT3 appears to promote aberrant proliferation and survival of hematopoietic stem/progenitor cells, leading to leukemogenesis (Kelly *et al.*, 2002).

Because of the high frequency of mutations and overexpression, FLT3 should be an appropriate therapeutic target in AML (Griffin, 2004). It has been shown that the staurosporine derivative PKC412 inhibits multi-target tyrosine kinases, including FLT3, protein kinase C, CDC2 and receptors for PDGF, FGF and VEGF (Levis and Small, 2005). PKC412 induces apoptosis in blasts from AML patients with FLT3 mutations, and prolongs survival in animal models of FLT3-induced myeloproliferative diseases (Weisberg *et al.*, 2002). Clinical trials for patients with solid tumors and AML revealed that PKC412 alone yielded limited clinical activity (Propper *et al.*, 2001; Stone *et al.*, 2005). To overcome this limitation, it is reasonable to combine PKC412 with other conventional antileukemic agents.

Recently, we have reported that PKC412 has synergistic effects with most antileukemic agents for FLT3-mutated leukemia cell lines (Furukawa *et al.*, 2007). In contrast, PKC412 is antagonistic to most drugs, except for those inducing mitotic arrest or active in the G_2/M phase in leukemia cell lines without FLT3 mutations. This finding provides useful information for the design of effective combination therapy containing PKC412. For safe and effective clinical applications, however, it is essential to clarify the molecular basis of the FLT3 mutation-dependent divergence of leukemic cell responses to PKC412. In this study, we attempted to resolve this issue by analysing the effects of PKC412 on the expression of cell cycle regulators and Bcl-2 family proteins in AML cell lines with or without FLT3 mutations.

Correspondence: Professor Y Furukawa, Division of Stem Cell Regulation, Center for Molecular Medicine, Jichi Medical School, 3311-1 Yakushiji, Shimotsuke, Tochigi 329-0498, Japan.
E-mail: furuyu@jichi.ac.jp
Received 2 July 2007; revised 5 November 2007; accepted 6 November 2007; published online 10 December 2007

Results

Effects of PKC412 on growth kinetics of AML cell lines with or without FLT3 mutations

We first compared the sensitivity to PKC412 of four AML cell lines: MOLM13, MV4-11, THP-1 and U937. It has been shown that MOLM13 and MV4-11 cell lines carry FLT3-ITD (internal tandem duplication), whereas FLT3 is in wild-type configuration in THP-1 and U937 cell lines (Quentmeier *et al*., 2003). THP-1 cells express a large amount of FLT3 but U937 cells do not express FLT3 (Yao *et al*., 2003). In pilot experiments, we determined the dose–response curves at day 3 (data not shown), and calculated the IC_{50} values for MOLM13, MV4-11, THP-1 and U937 to be 38 ± 4, 34 ± 6, 116 ± 26 and 207 ± 41 nM, respectively. On the basis of this result, we treated these cell lines with 100 nM PKC412 and observed the changes in growth kinetics. As shown in Figure 1a, PKC412 almost completely inhibited an increase in cell numbers of MOLM13 and MV4-11 cell lines. Growth inhibition was accompanied by the abrogation of constitutive phosphorylation of FLT3 (Figure 1b). The effects of PKC412 on other possible targets were variable and not correlated with cytotoxicity (Figure 1c and Supplementary Figure 1), suggesting that FLT3 is a principal target of PKC412-mediated growth inhibition of MOLM13 and MV4-11 cells. The proliferation of THP-1 cells was also markedly suppressed by PKC412, whereas U937 cells were relatively resistant to the drug (Figure 1a, lower panel). It is of note that the steady-state growth of AML cell lines with FLT3 mutations (MOLM13 and MV4-11) was significantly slower than that of AML cell lines without FLT3 mutations (THP-1 and U937) (Figure 1a, upper panel).

Cell cycle analysis of PKC412-treated AML cell lines

Next, we attempted to clarify the underlying mechanisms of PKC412-mediated growth inhibition of AML cell lines using cell cycle analysis. PKC412-induced apoptosis, as judged by an increase in the size of the sub-G_1 fraction (see Figure 2a for representative results, and Table 1 for quantification and statistical analysis of three independent experiments), DNA fragmentation (Figure 2b) and the appearance of apoptotic bodies (Figure 2c), in MOLM13 and MV4-11 cell lines after 24 h of culture without markedly affecting cell cycle distribution except for a minor decrease in the fraction of cells in the growth phases (S and G_2/M phases). In contrast, THP-1 and U937 cells were arrested in the G_2 phase by PKC412 after 12 h of treatment, and underwent mitotic slippage to become hyperploid after 48 h, especially in the latter (Figure 2 and Table 1). Apoptosis was barely observed in these cell lines up to 48 h of culture.

The difference of the changes in cell cycle distribution between PKC412-treated AML cell lines with FLT3-ITD and those with wild-type FLT3 may provoke the differential responses of cells to the combination of PKC412 and cell cycle-modifying drugs. To verify this

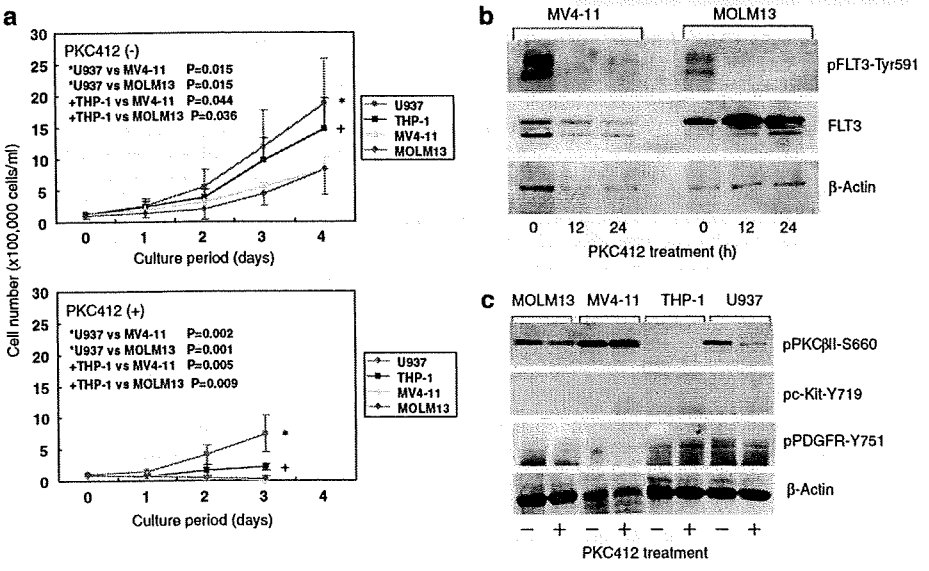

Figure 1 Effects of PKC412 on cell growth and FLT3 phosphorylation of acute myeloblastic leukemia (AML) cell lines. (**a**) We seeded AML cell lines at an initial concentration of 1×10^5 cells ml^{-1}, and cultured in the absence (upper panel) or presence (lower panel) of 100 nM PKC412 for up to 4 days. Viable cells were counted after staining with erythrosine B dye. The means ± s.d. (bars) of three independent experiments are shown. Statistical analysis was performed using Student's *t*-test. (**b**) Whole cell lysates were prepared from MV4-11 and MOLM13 cells cultured with 100 nM PKC412 at the indicted time points, and subjected to immunoblotting with an antibody that specifically recognizes FLT3 phosphorylated at tyrosine-591 (pFLT3-Tyr591). The membranes were reblotted with anti-FLT3 and β-actin antibodies to serve as loading controls. (**c**) Whole cell lysates were prepared from four cell lines before (−) and after (+) culture with 100 nM PKC412 for 24 h, and used for the detection of the indicated proteins. Data shown are representative of multiple independent experiments.

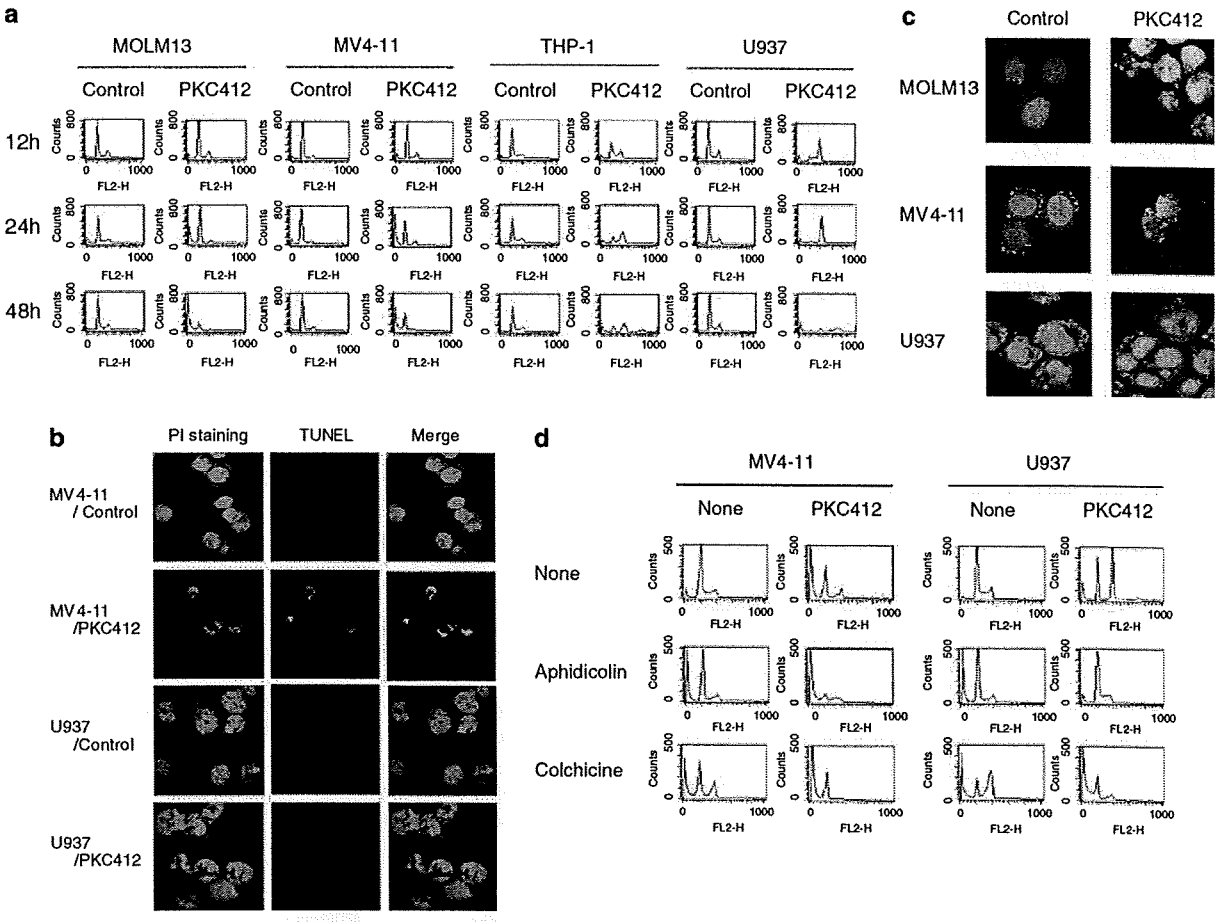

Figure 2 Differential effects of PKC412 on the cell cycle of acute myeloblastic leukemia (AML) cell lines with or without FLT3 mutations. MOLM13, MV4-11, THP-1 and U937 cells were seeded at 1×10^5 cells ml^{-1}, and cultured in the absence (control) or presence (PKC412) of 100 nM PKC412. (**a**) Cells were harvested at the indicated time points, and stained with propidium iodide in preparation for cell cycle analysis. See Table 1 for quantification and statistical analysis. (**b**) After 24 h of culture, cells were harvested for the detection of DNA fragmentation by the TUNEL method. Fragmented DNA was labeled with biotin-dUTP and stained with avidin-conjugated fluorescein isothiocyanate (FITC; TUNEL). Intact DNA was counterstained with propidium iodide (PI staining). Original magnification is ×400 for all panels. (**c**) After 24 h of culture, cells were stained with an antitubulin antibody (green fluorescence) and propidium iodide (red fluorescence). Original magnification is ×600 for all panels. (**d**) MV4-11 and U937 cells were cultured with (aphidicolin and colchicine) or without (none) cell cycle-modifying drugs in the absence (none) or presence (PKC412) of PKC412. The concentrations of each drug were PKC412 100 nM, aphidicolin 1 mg ml^{-1} and colchicine 100 nM. After 24 h of culture, cells were harvested for cell cycle analysis. The data shown are representative of three independent experiments.

hypothesis, we examined the combined effects of PKC412 and either aphidicolin, which induces G_1/S arrest by inhibiting DNA polymerase α, or colchicine, which arrests cells at mitosis by disrupting mitotic spindle. As shown in Figure 2d, PKC412 was synergistic with both aphidicolin and colchicine in MV4-11 cells, but only with colchicine in U937 cells. This is fully consistent with the pattern of cell cycle changes induced by PKC412 in each cell line.

PKC412 differentially modulates the phosphorylation of CDC2 in AML cell lines depending on the presence of FLT3 mutations

The above results indicate that PKC412 inhibits the growth of AML cells via distinct mechanisms depending on the presence of FLT3 mutations. We investigated the underlying mechanisms of differential responses to PKC412. First, we checked the phosphorylation status of CDC2, which reflects its activity *in vivo*, in PKC412-treated AML cell lines. As shown in Figure 3a, CDC2 was heavily phosphorylated at tyrosine-15, an ATP-binding site critical for the kinase function of CDC2 (Watanabe *et al.*, 1995), in untreated MOLM13 and MV4-11 cells. In contrast, CDC2-tyrosine 15 phosphorylation was not prominent in untreated THP-1 and U937 cells. These results suggest that CDC2 is relatively inactive in AML cell lines with FLT3 mutations, but is constitutively active in AML cell lines with wild-type FLT3. This pattern is fully compatible with the steady-state growth kinetics of these cells (Figure 1a). PKC412 modified the phosphorylation state of CDC2 in a reciprocal manner dependent on the presence of FLT3 mutations: CDC2 phosphorylation decreased

Table 1 Effects of PKC412 on cell cycle distribution of acute myeloblastic leukemia (AML) cell lines[a]

	MOLM13			*MV4-11*			*THP-1*			*U937*		
	Control	*PKC412*	P-*value**	*Control*	*PKC412*	P-*value**	*Control*	*PKC412*	P-*value**	*Control*	*PKC412*	P-*value**
12 h												
Sub-G_1	4.6±0.9	9.7±3.2	**0.04880**	5.6±0.8	6.8±1.7	0.21342	3.7±0.7	6.3±1.0	0.06957	3.7±0.8	3.3±0.8	0.21961
G_1	79.1±1.4	73.7±5.4	0.15931	82.6±3.2	81.2±1.8	0.36663	71.7±6.3	61.2±2.0	0.10660	79.3±2.2	22.1±3.4	**0.00022**
S+G_2/M	16.3±0.9	16.6±3.0	0.46585	11.8±2.5	12.0±2.7	0.47673	24.5±5.7	32.5±1.9	0.13740	17.1±2.6	74.6±4.2	**0.00023**
24 h												
Sub-G_1	7.8±0.7	14.4±2.9	**0.02911**	6.8±1.6	31.3±3.3	**0.00974**	2.6±0.7	3.8±0.7	0.13211	3.7±1.0	3.2±0.8	0.35510
G_1	72.0±1.8	79.2±2.8	**0.00553**	82.0±0.6	56.7±3.8	**0.00734**	67.8±2.0	27.6±3.2	**0.00406**	76.3±3.3	9.4±1.4	**0.00091**
S+G_2/M	20.2±1.3	6.4±0.8	**0.00384**	11.3±1.1	12.0±0.6	0.13694	29.6±2.5	68.5±3.7	**0.00632**	20.0±2.5	87.5±1.3	**0.00046**
48 h												
Sub-G_1	3.2±0.5	75.3±2.1	**0.00032**	4.4±1.4	59.2±3.5	**0.00196**	3.3±1.1	6.0±2.3	0.05624	4.6±0.7	5.7±1.5	0.09568
G_1	78.7±1.8	17.1±1.7	**0.00024**	84.1±3.6	34.3±1.9	**0.00299**	67.7±2.1	19.8±3.1	**0.00292**	76.3±3.2	8.8±2.5	**0.00046**
S+G_2/M	18.1±1.4	7.6±3.1	**0.00942**	11.5±2.6	6.5±1.7	**0.04318**	28.9±2.8	74.2±4.0	**0.00393**	19.0±4.0	85.5±3.5	**0.00033**

**P*-value was obtained by a paired Student's *t*-test between the data from untreated (control) and PKC412-treated (PKC412) cells ($n=3$). Data are the means±s.d. of three independent experiments. Bold values indicate $P<0.05$. [a]The proportion of cells in each phase of the cell cycle was calculated with the ModFitLT 2.0 program.

in MOLM13 and MV4-11, and increased in THP-1 and U937 after treatment with the drug. The inhibition of CDC2 kinase activity may underlie PKC412-induced G_2 arrest of THP-1 and U937 cells.

As Myt-1 kinase is responsible for CDC2 phosphorylation at tyrosine-15 (Galaktionov *et al.*, 1995), we examined the activation status of Myt-1 in these cells by immunoblotting with an antibody specifically recognizing the inactive/phosphorylated species of Myt-1. Consistent with the phosphorylation status of CDC2, Myt-1 was active (underphosphorylated) in AML cell lines with FLT3-ITD and inactive (phosphorylated) in AML cell lines without FLT3-ITD before treatment with PKC412 (Figure 3a). Myt-1 became phosphorylated and thereby inactivated by PKC412 in the former, whereas it became dephosphorylated and thereby activated in the latter, leading to the increased phosphorylation of CDC2. It is of note that Wee1, another kinase involved in tyrosine-15 phosphorylation, was below the detection limit in FLT3 mutation-positive leukemic cells as previously described (Neben *et al.*, 2005).

Next, we investigated the effects of PKC412 on the activity and intracellular localization of CDC25c, which activates CDC2 by removing phosphates from tyrosine-15. CDC25c was phosphorylated at serine-216 in untreated MOLM13 and MV4-11 cells, and was dephosphorylated by PKC412 (Figure 3a). In contrast, PKC412 increased the serine-216 phosphorylation of CDC25c in THP-1 and U937 cells. Upon phosphorylation at serine-216, CDC25c binds to 14-3-3 proteins and is translocated from the nucleus to the cytoplasm (Lopez-Girona *et al.*, 1999). We therefore confirmed the cytoplasmic sequestration of CDC25c phosphorylated at serine-216 using immunocytochemistry. As shown in Figure 3b, CDC25c was mostly retained in the cytoplasm in untreated MOLM13 cells, and was translocated to the nucleus after treatment with PKC412. In contrast, CDC25c was distributed throughout the entire cells in untreated U937 cells, and became sequestered in the cytoplasm and thus inactivated by the addition of PKC412. These observations are fully consistent with the pattern of serine-216 phosphorylation shown in Figure 3a. Furthermore, we demonstrated the binding of phosphorylated CDC25c to 14-3-3 proteins in cytoplasm using confocal microscopy. As shown in Figure 3c, phosphorylated CDC25c colocalized with 14-3-3 in untreated MV4-11 cells, and the interaction was dissociated after culture with PKC412. In U937 cells, PKC412 increased the amounts of phosphorylated CDC25c, which translocated from the nucleus and bound to 14-3-3 proteins in the cytoplasm. These results at least partly explain why PKC412 arrests cells in the G_2 phase of the cell cycle exclusively in AML cell lines without FLT3 mutations.

PKC412-induced apoptosis of AML cell lines with FTL3 mutations is mediated via selective phosphorylation of Bad at serine-128

Finally, we attempted to clarify the molecular mechanisms by which only AML cells with FLT3 mutations underwent apoptosis in the presence of PKC412. To this end, we screened for the expression of proapoptotic members of the Bcl-2 family by immunoblotting. As the expression of Bax and Bak was constitutive and unaffected by PKC412 in four AML cell lines (data not shown), we focused on BH3-only members of the Bcl-2 family, direct inducers of apoptosis (Galonek and Hardwick, 2006; Green, 2006). Among BH3-only proteins examined, only Bad was moderately expressed, and Bim, Bid, Puma and Noxa were undetectable in AML cell lines used in this study (data not shown). As PKC412 did not change the abundance of Bad protein, we examined the phosphorylation status of Bad using phosphorylation site-specific antibodies. It has been shown that Bad phosphorylation at various residues represents a checkpoint for the cell fate decision. For instance, CDC2 enhances the proapoptotic ability of

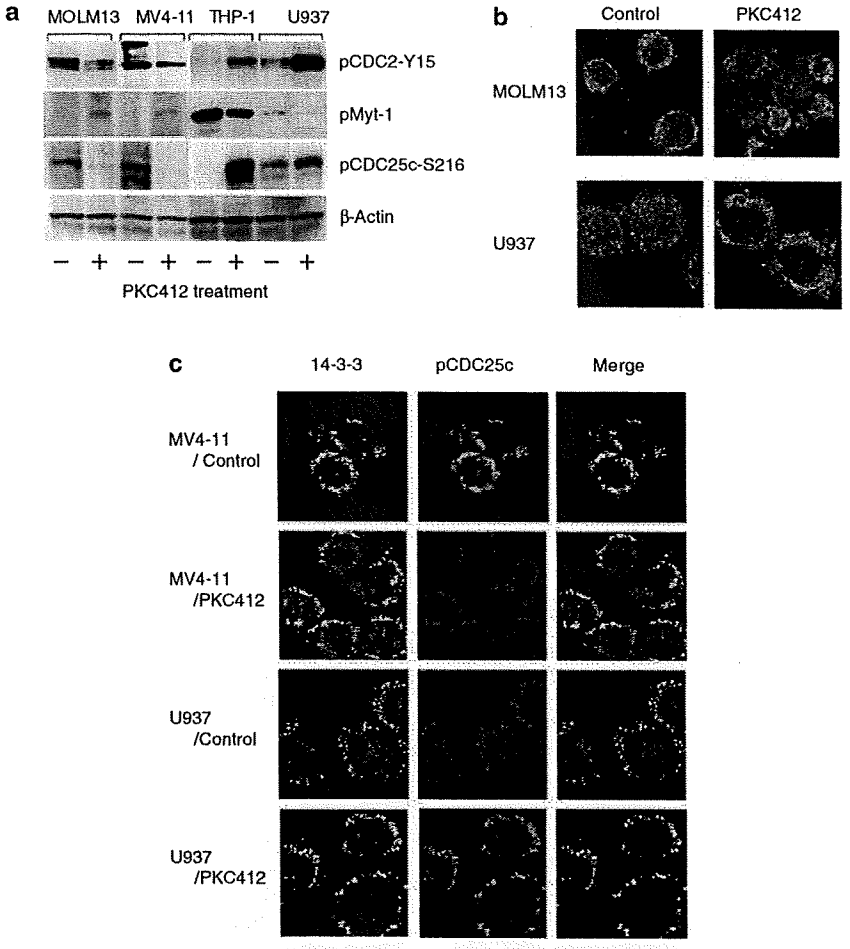

Figure 3 PKC412 differentially modulates CDC2 phosphorylation in acute myeloblastic leukemia (AML) cell lines depending on the presence of FLT3 mutations. **(a)** Whole cell lysates were prepared from AML cell lines before (−) and after (+) culture with 100 nM PKC412 for 24 h, and subjected to immunoblot analysis for the indicated proteins. **(b)** Intracellular localization of CDC25c was examined by immunocytochemistry in MOLM13 and U937 cells cultured in the absence (control) or presence (PKC412) of 100 nM PKC412 for 24 h. After being fixed, cells were stained with an anti-CDC25c monoclonal antibody and Alexa 488-conjugated goat antibody to mouse immunoglobulin. Original magnification is × 600 for all panels. **(c)** Colocalization of CDC25c and 14-3-3 proteins was examined by confocal microscopy in MV4-11 and U937 cells cultured in the absence (control) or presence (PKC412) of 100 nM PKC412 for 24 h. After being fixed, cells were stained with antibodies against 14-3-3 proteins and CDC25c phosphorylated at serine 216, followed by incubation with Alexa 488-conjugated goat antibody to mouse immunoglobulin and Cy3-conjugated goat antibody to rabbit immunoglobulin. Original magnification is × 600 for all panels. Data shown are representative of multiple independent experiments.

Bad by promoting serine-128 phosphorylation and mitochondrial translocation of Bad (Konishi *et al.*, 2002). In contrast, Akt promotes cell survival by phosphorylating Bad at serine-136, which provides a canonical binding site for 14-3-3 proteins to disrupt interaction with Bcl-2/Bcl-x on mitochondrial membranes (Zha *et al.*, 1996). Bad was phosphorylated at serine-136 and was inactive in untreated AML cells (Figure 4a, upper panel). Marginal levels of phosphorylation at serine-128 were observed in THP-1 and U937 cells, which may be due to the hyperactivation of CDC2. PKC412 induced Bad phosphorylation at serine-128 selectively in AML cell lines with FLT3-ITD along with dephosphorylation at serine-136 (Figure 4a, lower panel). AML cell lines with wild-type FLT3 did not show serine-128 phosphorylation. Next, we examined the intracellular localization of Bad using confocal microscopy. In untreated MV4-11 and U937 cells, Bad was distributed throughout the cytoplasm and did not colocalize with mitochondria (Figure 4b, Control). PKC412 induced the translocation of Bad to the mitochondria in MV4-11 cells but not in U937 cells (Figure 4b, PKC412). Intracellular localization of Bad is fully compatible with the alteration of site-specific phosphorylation of Bad, and at least partly explains the selective induction of apoptosis in AML cells with FLT3 mutations by PKC412.

Next, we determined the effects of PKC412 on the expression of antiapoptotic members of the Bcl-2 family. Immunoblot analyses revealed that AML cell lines used

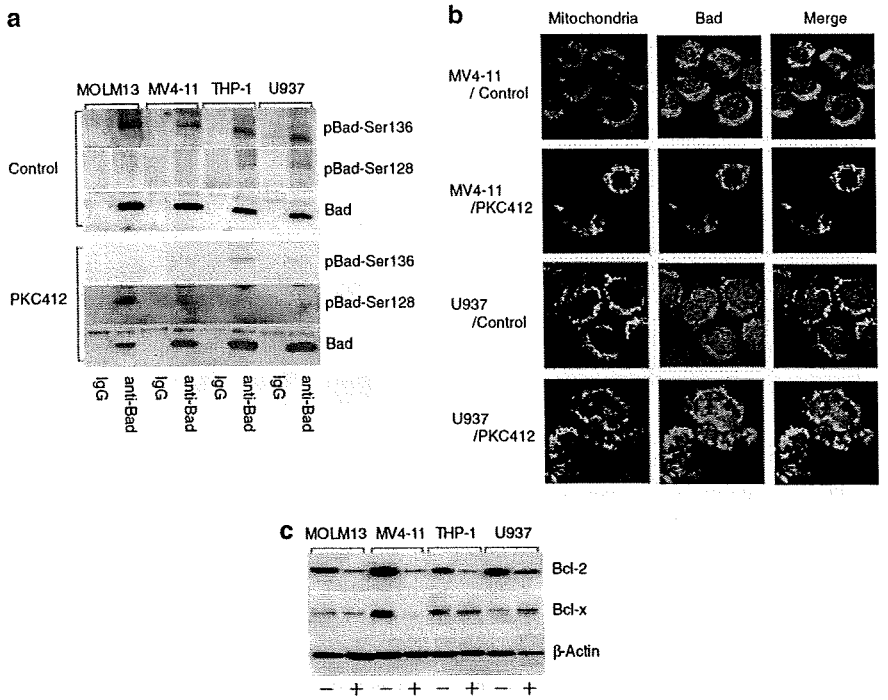

Figure 4 PKC412-induced apoptosis of acute myeloblastic leukemia (AML) cell lines with FTL3 mutations is mediated via phosphorylation of Bad at serine-128. (**a**) Whole cell lysates were prepared from AML cell lines cultured in the absence (control) or presence (PKC412) of 100 nM PKC412 for 24 h, and subjected to immunoprecipitation with either anti-Bad monoclonal antibody (anti-Bad) or mouse IgG (IgG). Immunoprecipitants were resolved on 12% acrylamide gels, followed by immunoblotting with polyclonal antibodies against Bad phosphorylated at serine-136, Bad phosphorylated at serine-128 and Bad. (**b**) For *in situ* visualization of Bad, we used anti-Bad polyclonal antibody and Cy3-conjugated goat antibody to rabbit immunoglobulin as primary and secondary antibodies, respectively. For co-labeling of mitochondria, we used a combination of anti-human mitochondria monoclonal antibody and Alexa 488-conjugated goat antibody to mouse immunoglobulin. (**c**) Protein samples in (**a**) were subjected to immunoblot analyses for Bcl-2, Bcl-x and β-actin (loading control). Data shown are representative of multiple independent experiments.

in this study expressed Bcl-2 and Bcl-x but not Mcl-1 and Bcl-w (data not shown). As shown in Figure 4c, Bcl-2 was readily downregulated by PKC412 in all four cell lines. The effects of PKC412 on Bcl-x expression were variable, suggesting that downregulation of Bcl-2 and Bcl-x is not a primary determinant of the sensitivity of AML cells to PKC412. However, it is possible that the reduced levels of Bcl-2 expression cooperate with the activation of Bad to enhance apoptosis in PKC412-treated MOLM13 and MV4-11 cells.

PKC412 induces apoptosis in primary AML cells with FTL3 mutations via the CDC2-Bad pathway

To testify the clinical relevance of our findings, we carried out the same experiments using primary AML cells from three patients with AML carrying FLT3-ITD. As shown in Figure 5a, PKC412 induced apoptosis with a decrease in the fraction of cells in the S phase in two cases and G_1 arrest with a moderate degree of apoptosis in one case. The effects of the drug on the phosphorylation status of FLT3, CDC2, Myt-1, CDC25c and Bad were almost identical to those observed in MOLM13 and MV4-11 cell lines (Figure 5b). There results indicate that our findings are not only valid in the cell line models, but have more general meanings.

Discussion

In this study, we obtained a clue pertinent to the molecular basis of the synergism and antagonism of PKC412 with other antileukemic agents. PKC412 alone induced G_2 arrest but not apoptosis in AML cell lines without aberrant FLT3 activation (THP-1 and U937) at a clinically achievable concentration. Because of the ability to cause G_2 arrest, PKC412 is synergistic with drugs that are active in the G_2/M phase, such as colchicine, in these cell lines. This may be an important advantage for the usage of PKC412 over other FLT3 inhibitors, because such effects have not been demonstrated with other FLT3 inhibitors (Levis *et al.*, 2004; Yee *et al.*, 2004). For the same reason, PKC412 may be antagonistic with drugs that synchronize target cells in late G_1 to early S phase, such as aphidicolin, in FLT3 mutation-negative leukemias. In contrast, PKC412-induced massive apoptosis without markedly affecting cell cycle patterns in AML cell lines harboring FLT3 mutations, which may underlie the synergism of PKC412 with most antileukemic agents.

Next, we attempted to elucidate the underlying mechanisms whereby PKC412 differentially affects the cell cycle distribution depending on the presence of FLT3 mutations. We obtained evidence suggesting that

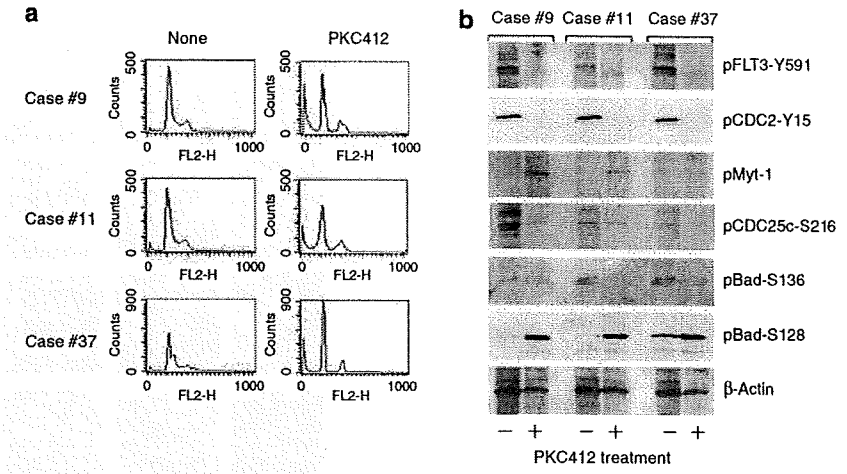

Figure 5 PKC412 induces apoptosis and cell cycle alterations in primary acute myeloblastic leukemia (AML) cells via the CDC2-Bad pathway. Bone marrow mononuclear cells from patients with AML carrying FLT3-ITD were cultured in the absence (none) or presence (PKC412) of 100 nM PKC412 for 24 h, and subjected to cell cycle analysis (**a**) and immunoblotting (**b**).

the cell cycle effect is mediated through the modulation of CDC2 activity by PKC412. The kinase activity of CDC2 is regulated by the opposing effects of specific kinases (Myt-1 and Wee1) and a specific phosphatase (CDC25c) on tyrosine-15, an ATP-binding site of CDC2 (Galaktionov *et al.*, 1995; Watanabe *et al.*, 1995). In untreated AML cell lines harboring FLT3-ITD, CDC2 was found to be at least partially inactivated by phosphorylation at tyrosine-15. This may be attributable to FLT3-ITD-mediated activation of Myt-1 kinase and inactivation of CDC25c by serine-216 phosphorylation and subsequent binding to 14-3-3 proteins. We are now trying to elucidate the signaling pathways of FLT3-ITD causing these changes. The partial inactivation of CDC2 may underlie the observation that AML cells with FLT3-ITD grow slower than those with wild-type FLT3. PKC412 reversed this process and activated CDC2 by promoting Myt-1 inactivation and facilitating nuclear translocation of CDC25c. In AML cells without FLT3-ITD, CDC2 is mostly in an active conformation and allows rapid cell cycling. PKC412 seems to inhibit CDC2 activity through CDC25c inactivation, which results in G_2 arrest. Although the precise mechanisms underlying this phenomenon are at present unknown, similar observations have been reported in non-small cell lung cancer and glioblastoma (Ikegami *et al.*, 1996; Begemann *et al.*, 1998).

Finally, we went on to identify target molecules responsible for selective induction of apoptosis in PKC412-treated AML cells with FLT3 mutations. To this end, we investigated the expression and function of Bcl-2 family proteins. Apoptotic cell death usually occurs through mitochondrial outer membrane permeabilization (MOMP), which is controlled by the balance between pro- and antiapoptotic members of the Bcl-2 family. Bad is a member of the BH3-only subfamily, and is known to promote MOMP by activating membrane-anchored proapoptotic Bcl-2 family proteins Bax and Bak (Galonek and Hardwick, 2006; Green, 2006). The function of Bad is tightly regulated by phosphorylation. For instance, the PI3 kinase-Akt pathway mediates phosphorylation of Bad at serine-136 and abrogates its proapoptotic activity (Zha *et al.*, 1996). It is well known that FLT3-ITD phosphorylates Bad through the Akt pathway and suppresses apoptosis of hematopoietic stem cells, which contribute to the development of leukemia (Kim *et al.*, 2006). In contrast, serine-128 phosphorylation promotes apoptosis in primary neurons by antagonizing survival functions of growth factors (Konishi *et al.*, 2002). Serine-128 phosphorylation is shown to be catalysed by CDC2 and c-Jun N-terminal kinase (Donovan *et al.*, 2002). Our results suggest that PKC412 causes phosphorylation of Bad at serine-128 via CDC2 activation along with dephosphorylation at serine-136 via blocking FLT3-ITD signaling, which results in apoptosis of AML cells with FLT3 mutations. In AML cells without FLT3-ITD, Bad phosphorylation at serine-128 did not occur because of PKC412-mediated inactivation of CDC2. Although serine-136 was dephosphorylated in some degree, these cells did not undergo apoptosis in response to PKC412. This is in line with a previous report that dephosphorylation of Bad is not sufficient and downregulation of Bcl-x is necessary for the induction of apoptosis (Yang *et al.*, 2005). In addition, Bcl-x inhibits CDC2 kinase activity at the G_2/M checkpoint by direct binding and causes G_2 arrest (Schmitt *et al.*, 2007). As Bcl-x was not downregulated in PKC412-treated THP-1 and U937 cells, it is possible that Bcl-x serves as an additional factor to determine the responses to PKC412.

Materials and methods

Reagents

PKC412 was purchased from LC Laboratories (Woburn, MA, USA), dissolved in dimethyl sulfoxide and stored at −20 °C until use.

Cells and cell culture
We used four human AML cell lines, that is, MOLM13, derived from a patient with acute monocytic leukemia (AMoL) carrying t(9;11); MV4-11, derived from a patient with AMoL carrying t(4;11); THP-1 and U937, derived from patients with AMoL without FLT3 mutations. MV4-11, THP-1 and U937 were purchased from the American Type Culture Collection (Manassas, VA, USA), and MOLM13 was provided by Dr Yoshinobu Matsuo (Grandsoul Research Institute for Immunology, Nara, Japan). These cell lines were maintained in RPMI1640 medium supplemented with 10% fetal bovine serum. Primary AML cells were isolated from the bone marrow of patients at the time of diagnostic procedure. Informed consent was obtained in accordance with the Declaration of Helsinki, and the protocol was approved by the institutional review board. The presence of FLT3-ITD was examined as described by Kiyoi *et al.* (1997).

Flow cytometric analysis
The cell cycle profile was obtained by staining DNA with Vindelov's solution (0.04 mg ml^{-1} propidium iodide in 5 mM Tris–HCl, 5 mM NaCl and 0.005% nonidet P-40) in preparation for flow cytometry. The size of the sub-G_1, G_0/G_1 and $S+G_2/M$ fractions was calculated as a percentage by analysing DNA histograms with the ModFitLT 2.0 program (Verity Software, Topsham, ME, USA). Surface marker analysis was carried out according to the standard method.

Immunocytochemistry
After collecting on glass slides using a Cytospin centrifugator (Shandon Scientific, Cheshire, England), cells were fixed in 4% paraformaldehyde in phosphate-buffered saline, and stained with a rabbit antitubulin polyclonal antibody (Sigma, St Louis, MO, USA) and Alexa 488-conjugated goat antibody to rabbit immunoglobulin (Molecular Probes, Eugene, OR, USA) as primary and secondary antibodies, respectively. Finally, nuclear DNA was stained with 100 ng ml^{-1} propidium iodide in phosphate-buffered saline for 5 min.

Detection of apoptosis
Apoptosis was detected *in situ* by the TUNEL (TdT-mediated dUTP-biotin nick end labeling) method using MEBSTAIN apoptosis kit (MBL International, Woburn, MA, USA). In brief, cells were fixed on glass slides as described above, and treated with terminal deoxynucleotidyl transferase (TdT) in the presence of biotin-dUTP to label 3′-ends of fragmented DNA. The labeled ends were visualized with avidin-conjugated fluorescein isothiocyanate (FITC). Finally, intact DNA was counterstained with propidium iodide.

Confocal laser microscopy
Confocal microscopic analysis was performed using the following antibodies: anti-CDC25c (C2-2; BD Pharmingen, San Jose, CA, USA), antiphosphorylated CDC25c at serine-216 (no. 4901; Cell Signalling Technology, Beverly, MA, USA), anti-human 14-3-3 (C23-1; BD Pharmingen), anti-Bad (no. 9292; Cell Signalling Technology) and anti-human mitochondria (AE-1; Leinco Technologies Inc., St Louis, MO, USA). We used Alexa 488-conjugated goat antibody to mouse immunoglobulin (Molecular Probes) and Cy3-conjugated goat antibody to rabbit immunoglobulin (Amersham Pharmacia Biotech, Piscataway, NJ, USA) as secondary antibodies.

Immunoprecipitation and immunoblotting
Immunoprecipitation and immunoblotting were carried out according to the standard methods using the following antibodies: anti-FLT3 (8F2; Santa Cruz Biotechnology, Santa Cruz, CA, USA), antiphosphorylated FLT3 at tyrosine-591 (no. 3461; Cell Signalling Technology), antiphosphorylated protein kinase C (pan) at serine-660 (no. 9371; Cell Signalling Technology), antiphosphorylated c-Kit at tyrosine-719 (no. 3391; Cell Signalling Technology), antiphosphorylated PDGF receptor β at tyrosine-751 (no. 3161; Cell Signalling Technology), antiphosphorylated CDC2 at tyrosine-15 (no. 9111; Cell Signalling Technology), anti-Bad monoclonal (clone 48; BD Transduction Laboratories, San Jose, CA, USA), anti-Bad polyclonal (no. 9292; Cell Signalling Technology), antiphosphorylated Bad at serine-136 (no. 9295; Cell Signalling Technology), antiphosphorylated Bad at serine-128 (AB3567; Chemicon International, Temecula, CA, USA), anti-Bcl-2 (clone 4D7; BD Transduction Laboratories), anti-Bcl-x (clone 44; BD Transduction Laboratories) and anti-β-actin (C4; ICN Biomedicals, Aurora, OH, USA).

Acknowledgements

This work was supported in part by the High-Tech Research Center Project for Private Universities: Matching Fund Subsidy from MEXT 2002–2006, and grants from the Vehicle Racing Commemorative Foundation and Sankyo Foundation of Life Science (to YF). JK is a winner of the Jichi Medical School Young Investigator Award. TW is a winner of the Jichi Medical School Graduate Student Award.

References

Begemann M, Kashimawo SA, Heitjan DF, Schiff PB, Bruce JN, Weinstein IB. (1998). Treatment of human glioblastoma cells with the staurosporine derivative CGP 41251 inhibits CDC2 and CDK2 kinase activity and increases radiation sensitivity. *Anticancer Res* **18**: 2275–2282.

Donovan N, Becker EB, Konishi Y, Bonni A. (2002). JNK phosphorylation and activation of BAD couples the stress-activated signaling pathway to the cell death machinery. *J Biol Chem* **277**: 40944–40949.

Furukawa Y, Vu HA, Akutsu M, Odgerel T, Izumi T, Tsunoda S *et al.* (2007). Divergent cytotoxic effects of PKC412 in combination with conventional antileukemic agents in FLT3 mutation-positive versus negative leukemia cell lines. *Leukemia* **21**: 1005–1014.

Galaktionov K, Jessus C, Beach D. (1995). Raf1 interaction with Cdc25 phosphatase ties mitogenic signal transduction to cell cycle activation. *Genes Dev* **9**: 1046–1058.

Galonek HL, Hardwick JM. (2006). Upgrading the bcl-2 network. *Nat Cell Biol* **12**: 1317–1319.

Gilliland DG, Griffin JD. (2002). The roles of FLT3 in hematopoiesis and leukemia. *Blood* **100**: 1532–1542.

Green DR. (2006). At the gates of death. *Cancer Cell* **9**: 328–330.

Griffin JD. (2004). FLT3 tyrosine kinase as a target in acute leukemias. *Hematol J* **5**: 188–190.

Ikegami Y, Yano S, Nakao K. (1996). Effects of the new selective protein kinase C inhibitor 4′-N-benzoyl staurosporine on cell cycle distribution and growth inhibition in human small cell lung cancer cells. *Arzneimittelforschung* **46**: 201–204.

Kelly LM, Liu Q, Kutok JL, Williams IR, Boulton CL, Gilliland DG. (2002). FLT3 internal tandem duplication mutations associated with human acute myeloid leukemias induce myeloproliferative disease in a murine bone marrow transplant model. *Blood* **99**: 310–318.

Kim KT, Levis M, Small D. (2006). Constitutively activated FLT3 phosphorylates BAD partially through pim-1. *Br J Haematol* **134**: 500–509.

Kiyoi H, Naoe T, Yokota S, Nakao M, Minami S, Kuriyama K *et al.* (1997). Internal tandem duplication of FLT3 associated with leukocytosis in acute promyelocytic leukemia. *Leukemia* **11**: 1447–1452.

Konishi Y, Lehtinen M, Donovan N, Bonni A. (2002). Cdc2 phosphorylation of BAD Links the cell cycle to the cell death machinery. *Mol Cell* **9**: 1005–1016.

Levis M, Pham R, Smith BD, Small D. (2004). *In vitro* studies of a FLT3 inhibitor combined with chemotherapy: sequence of administration is important to achieve synergistic cytotoxic effects. *Blood* **104**: 1145–1150.

Levis M, Small D. (2005). FLT3 tyrosine kinase inhibitors. *Int J Hematol* **82**: 100–107.

Lopez-Girona A, Furnari B, Mondesert O, Russell P. (1999). Nuclear localization of Cdc25 is regulated by DNA damage and a14-3-3 protein. *Nature* **397**: 172–175.

Lyman SD, James L, Vanden Bos T, de Vries P, Brasel K, Gliniak B *et al.* (1993). Molecular cloning of a ligand for the flt3/flk-2 tyrosine kinase receptor: a proliferative factor for primitive hematopoietic cells. *Cell* **75**: 1157–1167.

Neben K, Schnittger S, Bross B, Tews B, Kokocinski F, Haferlach T *et al.* (2005). Distinct gene expressions patterns associated with FLT3- and NRAS- activating mutations in acute myeloid leukemia with normal karyotype. *Oncogene* **24**: 1580–1588.

Propper DJ, McDonald AC, Man A, Thavasu P, Balkwill F, Braybrooke JP *et al.* (2001). Phase I and pharmacokinetic study of PKC412, an inhibitor of protein kinase C. *J Clin Oncol* **19**: 1485–1492.

Quentmeier H, Reinhardt J, Zaborski M, Drexler HG. (2003). FLT3 mutations in acute myeloid leukemia cell lines. *Leukemia* **17**: 120–124.

Schmitt E, Beauchemin M, Bertrand R. (2007). Nuclear colocalization and interaction between bcl-xL and cdk1 (cdc2) during G2/M cell-cycle checkpoint. *Oncogene* **26**: 5851–5865.

Small D, Levenstein M, Kim E, Carow C, Amin S, Rockwell P *et al.* (1994). STK-1, the human homolog of Flk-2/Flt-3, is selectively expressed in CD34$^+$ human bone marrow cells and is involved in the proliferation of early progenitor/stem cells. *Proc Natl Acad Sci USA* **91**: 459–463.

Stone RM, DeAngelo DJ, Klimek V, Galinsky I, Estey E, Nimer SD *et al.* (2005). Patients with acute myeloid leukemia and an activating mutation in FLT3 respond to a small-molecule FLT3 tyrosine kinase inhibitor, PKC412. *Blood* **105**: 54–60.

Watanabe N, Broome M, Hunter T. (1995). Regulation of the human Wee1 CDK tyrosine 15 kinase during cell cycle. *EMBO J* **14**: 1878–1891.

Weisberg E, Boulton C, Kelly LM, Manley P, Fabbro D, Meyer T *et al.* (2002). Inhibition of mutant FLT3 receptors in leukemia cells by the small molecule tyrosine kinase inhibitor PKC412. *Cancer Cell* **1**: 433–443.

Yang X, Lui L, Sternberg D, Tang L, Galinsky I, DeAngelo D *et al.* (2005). The FLT3 internal tandem duplication mutation prevents apoptosis in interleukin 3-deprived BaF3 cells due to protein kinase A and ribosomal S6 Kinase 1-mediated BAD phosphorylation at serine 112. *Cancer Res* **65**: 7338–7347.

Yao Q, Nishiuchi R, Li Q, Kumar AR, Hudson WA, Kersey JH. (2003). FLT3 expressing leukemias are selectively sensitive to inhibitors of the molecular chaperone heat shock protein 90 through destabilization of signal transduction-associated kinases. *Clin Cancer Res* **9**: 4483–4493.

Yee KW, Schittenhelm M, O'Farrell AM, Town AR, McGreevey L, Bainbridge T *et al.* (2004). Synergistic effect of SU11248 with cytarabine or daunorubicin on FLT3 ITD-positive leukemic cells. *Blood* **104**: 4202–4209.

Zha J, Harada H, Yang F, Jockel J, Korsmeyer SJ. (1996). Serine phosphorylation of death agonist Bad in response to survival factor results in binding to 14-3-3 not BCL-XL. *Cell* **87**: 619–628.

Supplementary Information accompanies the paper on the Oncogene website (http://www.nature.com/onc).

European Journal of Haematology 83 (90–98)

ORIGINAL ARTICLE

Comprehensive analysis of cooperative gene mutations between class I and class II in *de novo* acute myeloid leukemia

Yuichi Ishikawa[1,2], Hitoshi Kiyoi[1], Akane Tsujimura[1,2], Shuichi Miyawaki[3], Yasushi Miyazaki[4], Kazutaka Kuriyama[5], Masao Tomonaga[4], Tomoki Naoe[2]

[1]Department of Infectious Diseases and [2]Department of Hematology and Oncology, Nagoya University Graduate School of Medicine, Nagoya; [3]Leukemia research center, Saiseikai Maebashi Hospital, Maebashi; [4]Department of Hematology, Nagasaki University School of Medicine, Nagasaki; [5]Department of Hematoimmunology, School of Health Sciences, Faculty of Medicine, University of the Ryukyus, Nishihara, Japan

Abstract

Acute myeloid leukemia (AML) has been thought to be the consequence of two broad complementation classes of mutations: class I and class II. However, overlap-mutations between them or within the same class and the position of *TP53* mutation are not fully analyzed. We comprehensively analyzed the *FLT3, cKIT, N-RAS, C/EBPA, AML1, MLL, NPM1,* and *TP53* mutations in 144 newly diagnosed *de novo* AML. We found 103 of 165 identified mutations were overlapped with other mutations, and most overlap-mutations consisted of class I and class II mutations. Although overlap-mutations within the same class were found in seven patients, five of them additionally had the other class mutation. These results suggest that most overlap-mutations within the same class might be the consequence of acquiring an additional mutation after the completion both of class I and class II mutations. However, mutated genes overlapped with the same class were limited in *N-RAS, TP53, MLL*-PTD, and *NPM1*, suggesting the possibility that these irregular overlap-mutations might cooperatively participate in the development of AML. Notably, *TP53* mutation was overlapped with both class I and class II mutations, and associated with morphologic multilineage dysplasia and complex karyotype. The genotype consisting of complex karyotype and *TP53* mutation was an unfavorable prognostic factor in entire AML patients, indicating this genotype generates a disease entity in *de novo* AML. These results collectively suggest that *TP53* mutation might be a functionally distinguishable class of mutation.

Key words acute myeloid leukemia; overlap mutations; TP53; multilineage dysplasia; prognosis

Correspondence Hitoshi Kiyoi, MD, PhD, Department of Infectious Diseases, Nagoya University School of Medicine, 65 Tsurumai-cho, Showa-ku, Nagoya 466-8560, Japan. Tel: +81 52 744 2955; Fax: +81 52 744 2801; e-mail: kiyoi@med.nagoya-u.ac.jp

This study was supported by Grants-in-Aid from National Institute of Biomedical Innovation, the Ministry of Health, Labor and Welfare and the Scientific Research of the Ministry of Education, Culture, Sports, Science and Technology, Japan.

Accepted for publication 18 March 2009

doi:10.1111/j.1600-0609.2009.01261.x

Acute myeloid leukemia (AML) is a genetically and phenotypically heterogeneous disease (1). In 1999, the third edition of the World Health Organization (WHO) classification of the myeloid neoplasms classified AML into four major categories: AML with recurrent genetic abnormalities (AML-RGA), AML with multilineage dysplasia (AML-MLD), AML, therapy-related, and AML not otherwise categorized (2). The first category included AML with t(8;21)(q22;q22), (*AML1/ETO*), inv(16)(p13q22) or t(16;16)(p13;q22), (*CBFB/MYH11*), t(15;17)(q22;q12), (*PML/RARA*) and 11q23 (*MLL*) abnormalities, which create fusion genes associated with leukemogenesis. Each balanced translocation corresponded to characteristic cytogenetical and clinical

features. These translocations can be detected by reverse transcriptase-mediated PCR (RT-PCR), which becomes a sensitive, rapid and objective method for diagnosis (3). However, the classification of other categories is based on morphology of bone marrow (BM) cells and on the history of patients, although a number of genetic alterations, which are involved in the pathogenesis of AML and associated with the prognosis of patients, have been documented (4). Recently, it has been demonstrated that mutations of *FLT3*, *NPM1*, and *C/EBPA* genes are preferentially found in AML with normal cytogenetics and are highly implicated in the prognosis (5). The fourth edition of the WHO classification have included *NPM1* and *C/EBPA* mutations as provisional entities in AML-RGA, but not *FLT3* mutation because it is associated with a number of other entities (6). Furthermore, the AML-MLD category has been renamed as AML with myelodysplasia-related changes, in which myelodysplastic syndrome (MDS)-related cytogenetic abnormality, as well as previous history of MDS and MLD, has been included as a criteria for the diagnosis. However, it was suggested that AML is the consequence of two broad complementation classes of mutations: those that confer a proliferative and/or survival advantage to hematopoietic progenitors (class I mutation) and those that impair hematopoietic differentiation and confer properties of self-renewal (class II mutation) (7). In addition, clinical significance of genetic alterations in the setting of morphologic MLD remains unclear. Therefore, it is necessary to analyze genetic alterations comprehensively, taking them into account all together rather than individually to elucidate the genetic background and prognostic impact in AML (8).

It has been generally considered that *FLT3*, *cKIT*, and *N-RAS* mutations are class I mutations, and *C/EBPA* and *AML1* mutations, and *AML1/ETO*, *CBFB/MYH11*, *PML/RARA*, and *MLL* abnormalities are class II mutations, while overlap mutations of these mutations between class I and class II or within the same class in a clinical sample are not fully characterized, and the positions of *NPM1* mutation and the partial tandem duplication of the *MLL* gene (*MLL*-PTD) remain unclear. *TP53* mutations are reportedly infrequent but are associated with a poor prognosis in *de novo* AML (9–11). In addition, an association between *TP53* mutations and complex karyotype in therapy-related MDS and AML has been reported (12, 13). However, the position of *TP53* mutation remains unclear.

In this study, we comprehensively analyzed mutations of *FLT3*, *cKIT*, *N-RAS*, *C/EBPA*, *AML1*, *MLL*, *NPM1*, and *TP53* genes as well as cytogenetics in newly diagnosed *de novo* AML to disclose the feature of their overlap mutations. Furthermore, we examined the association of cooperative mutations with clinical characteristics and morphologic MLD of *de novo* AML.

Patients and methods

Patients and samples

The diagnosis of AML was based on the WHO classification. All BM smears from patients were evaluated by the authors according to the WHO criteria and morphological diagnosis was confirmed. The study population included 144 newly diagnosed *de novo* AML patients from January 1990 who were received the remission induction therapy in our institutes. We unselectively included all patients into the present study if their samples were available. The median age and WBC count at the diagnosis of the analyzed patients were 52 yr (range, 15–85 yr) and 10.3×10^9/L (range, $0.6–351 \times 10^9$/L), respectively. Twenty-one patients were of age 65 yr or older. Cytogenetic analysis revealed that a normal karyotype was found in 54 patients and an abnormal karyotype was in 90 patients including 19 t(8;21)(q22;q22), 3 inv(16)(p13q22), 14 t(15;17)(q22;q12) and 2 11q23 abnormalities. AML-MLD was identified in 34 patients, who did not have a history of MDS. BM samples from patients with AML were subjected to Ficoll-Hypaque (Pharmacia LKB, Uppsala, Sweden) density gradient centrifugation. Informed consent was obtained from all patients to use their samples for banking and molecular analysis, and approval was obtained from the ethics committee of Nagoya university school of medicine.

Therapy

Among the AML patients analyzed, patients younger than 65 yr old were treated with the AML protocols of the Japan Adult Leukemia Study Group or their modifications (14, 15). Briefly, the induction therapy consisted of cytarabine (Ara-C) and idarubicin (IDR) or Ara-C and daunorubicin (DNR). Patients who achieved complete remission (CR) subsequently received three courses of consolidation therapy consisted of high-dose Ara-C or four courses of consolidation consisted of Ara-C and mitoxantrone, Ara-C and DNR, Ara-C and aclarubicin, and Ara-C, etoposide, vincristine and vindesine. Patients aged 65 yr or older received the dose-reduced induction therapy consisted of Ara-C and IDR or Ara-C and DNR. For the consolidation therapy, four courses of the dose-reduced regimen were administered.

Cytogenetics analysis

The cytogenetic G-banding analysis was performed with standard methods. A complex karyotype was defined as

at least three unrelated chromosomal aberrations. Chimeric transcripts, *BCR/ABL*, *AML1/ETO*, *CBFB/MYH11*, *PML/RARA*, and *MLL/AF9*, were examined by real-time PCR as previously described (3).

Screening for mutations of *FLT3, cKIT, N-RAS, AML1, C/EBPA, TP53, MLL,* and *NPM1* genes

High-molecular-weight DNA and total RNA were extracted from the samples using standard methods. *FLT3* gene mutations of the internal tandem duplication in the juxtamembrane domain (FLT3/ITD) and deletion and point mutation in the kinase domain (FLT3/KDM), *NPM1* gene mutation of exon 12, *N-RAS* gene mutations of codons 12, 13, and 61 and *TP53* gene mutations of exons 5–8 were examined as reported and confirmed by the sequencing procedure (11, 16–19). The partial tandem duplication of the *MLL* gene (*MLL*-PTD) was examined by RT-PCR as described previously (17). Mutations of *AML1*, *C/EBPA* and exon 8, 10–11, and 17 of *cKIT* were screened by denaturing high performance liquid chromatography (DHPLC) analysis using the WAVE Maker System (Transgenomic Inc., San Jose, CA, USA) as reported (20–22). DHPLC gradients and temperatures were determined using WAVE Maker System software. When heterozygous profiles were identified by visual inspection of the chromatograms, mutations were confirmed by cloning and sequencing procedures as reported (20).

Statistical analysis

Differences in continuous variables were analyzed with the Mann–Whitney *U*-test for distribution among two groups or the Kruskal–Wallis test for distribution among more than two groups. Frequencies were analyzed using Fisher's exact test for 2×2 tables or Pearson's chi-squared test for larger tables. Multivariate analysis to identify risk factors for achieving CR was performed using the logistic-regression model. Survival probabilities were estimated by the Kaplan–Meier method, and differences in survival distributions were evaluated using the log-rank test. The prognostic significance of the clinical variables was assessed using the Cox proportional hazards model. These statistical analyses were performed with StatView-J 5.0 (Abacus Concepts Inc., Berkeley, CA, USA). For all analyses, the *P*-values were two-tailed, and a $P < 0.05$ was considered statistically significant.

Results

Mutations of *de novo* AML

Genetic alterations of AML patients according to cytogenetics are summarized in Table 1. At least one mutation in the *FLT3*, *cKIT*, *N-RAS*, *AML1*, *C/EBPA*, *MLL*, *NPM1*, *and TP53* genes was identified in 84 of the 144 AML patients (58.3%). *FLT3* mutation was the most frequently identified in entire AML patients (35/144, 24.3%), followed by *NPM1* (29/144, 20.1%) and *C/EBPA* (17/144, 11.8%) mutations. In *FLT3* mutation, FLT3/ITD and FLT3/KDM were identified in 28 (19.4%) and seven (4.9%) patients, respectively. No overlap mutation of FLT3/ITD and FLT3/KDM was observed. In cytogenetically normal AML, *NPM1* mutation was the most frequently identified (19/54, 35.2%), followed by FLT3/ITD (15/54, 27.8%) and *C/EBPA* (13/54, 24.1%) mutations. *FLT3* mutation was also frequently identified in AML with *PML/RARA*, *AML1/ETO*, or *CBFB/MYH11*, although *NPM1* and *C/EBPA* mutations were not. In contrast, *cKIT* mutation was not identified in cytogenetically normal AML, while it was frequently identified in AML with *AML1/ETO* (3/19, 15.8%) or *CBFB/MYH11* (1/3, 33.3%). When comparing cytogenetically normal and abnormal patients, *NPM1* and *C/EBPA* mutations were

Table 1 Genetic alterations of 144 *de novo* AML patients according to cytogenetics

	PML/RARA	AML1/ETO	CBFB/MYH11	MLL abnormalities	Normal	Other abnormalities	Complex	Total	*P*-value
Number	14	19	3	2	54	38	14	144	
Mutation (%)									
FLT3/ITD	3 (21.4)	0	1 (33.3)	0	15 (27.8)	8 (21.1)	1 (7.1)	28 (19.4)	NS
FLT3/KDM	0	2 (10.5)	0	0	3 (5.6)	2 (5.3)	0	7 (4.9)	NS
cKIT	0	3 (15.8)	1 (33.3)	0	0	4 (10.5)	0	8 (5.6)	0.0208
N-RAS	1 (7.1)	0	0	0	4 (7.4)	6 (15.8)	0	11 (7.6)	NS
TP53	0	1 (5.3)	0	0	1 (1.9)	1 (2.6)	8 (57.1)	11 (7.6)	<0.0001
NPM1	0	0	0	0	19 (35.2)	8 (21.1)	2 (14.3)	29 (20.1)	0.0076
MLL-PTD	0	1 (5.3)	1 (33.3)	1 (50)	5 (9.3)	3 (7.9)	2 (14.3)	13 (9.0)	NS
C/EBPA	0	0	0	0	13 (24.1)	2 (5.3)	2 (14.3)	17 (11.8)	0.0242
AML1	0	0	0	0	1 (1.9)	2 (5.3)	0	3 (2.1)	NS

Distributions of *cKIT*, *TP53*, *NPM1*, and *C/EBPA* mutations according to cytogenetics were significantly different.
AML, acute myeloid leukemia; NS, no significance.

frequently identified in cytogenetically normal patients (33.9% vs. 11.4%, $P = 0.0014$ and 23.2% vs. 4.5%, $P = 0.0011$, respectively). *TP53* mutation was identified in 11 AML patients (7.6%), and eight of them showed complex karyotype. As *AML1* mutation was identified in only three patients, further analysis is required to confirm the statistical significance of its distribution.

Overlap mutations

In the present study, we identified a total of 165 mutations in entire AML patients. Interestingly, 103 of the 165 mutations (62.4%) were overlapped with another mutations. *AML1* (3/3, 100%), FLT3/KDM (7/7, 100%), FLT3/ITD (24/28, 85.7%), *N-RAS* (9/11, 81.8%), and *NPM1* (21/29, 72.4%) mutations were frequently overlapped with another mutations. In contrast, overlap mutations of *PML/RARA* (3/14, 21.4%) and *AML1/ETO* (6/19, 31.6%) were relatively infrequent (Fig. 1A). The most frequent overlap mutation was *FLT3* and *NPM1*, which was observed in 16 of the 51 patients with overlap mutations, followed by *FLT3* and *MLL*-PTD (five patients), *FLT3* and *C/EBPA* (four patients), *FLT3* and *PML/RARA* (three patients), *cKIT* and *AML1/ETO* (three patients), *N-RAS* and *NPM1* (three patients) and *TP53* and *MLL*-PTD (three patients). Importantly, overlap pattern of mutations was not random as shown in Fig. 1(B). The overlap mutations of *FLT3* and *cKIT* were not identified. In addition, *PML/RARA*, *AML1/ETO*, *CBFB/MYH11*, and *MLL* gene abnormality and *AML1* and *C/EBPA* mutations were not overlapped each other. These results were consistent with the genetic model of class I and class II mutations. However, overlap patterns of *N-RAS*, *TP53*, *MLL*-PTD, and *NPM1* mutations seemed different from above mutations. *N-RAS* mutation was identified in nine patients, while each one of them were overlapped with FLT3/ITD and *cKIT* mutations, respectively. Likewise, overlap mutations of *TP53* and FLT3/ITD, *TP53* and *cKIT*, *MLL*-PTD and *AML1/ETO*, *MLL*-PTD and *CBFB/MYH11*, *MLL*-PTD and *MLL/ENL*, and *NPM1* and *C/EBPA* were found in each one patient. According to the general consideration that *N-RAS* and *TP53* mutations were the class I mutation, and *MLL*-PTD and *NPM1* mutations were the class II mutation, these overlap mutations seemed to irregularly occur within the same class. Taken together, overlap mutations in the same class were observed in seven patients, while five of them showed mutations in three different genes. In this study, 51 of the 144 patients (35.4%) revealed overlap mutations, and overlap mutations consisted of two or three genes were found in 46 and five patients, respectively. However, both class I and class II mutations were always included in all patients with three mutations (Table 2). Therefore, only two patients showed two mutations within the same class: one consisted of *N-RAS* and *cKIT* mutations and the other consisted of *MLL*-PTD and *MLL/ENL* (Table 2).

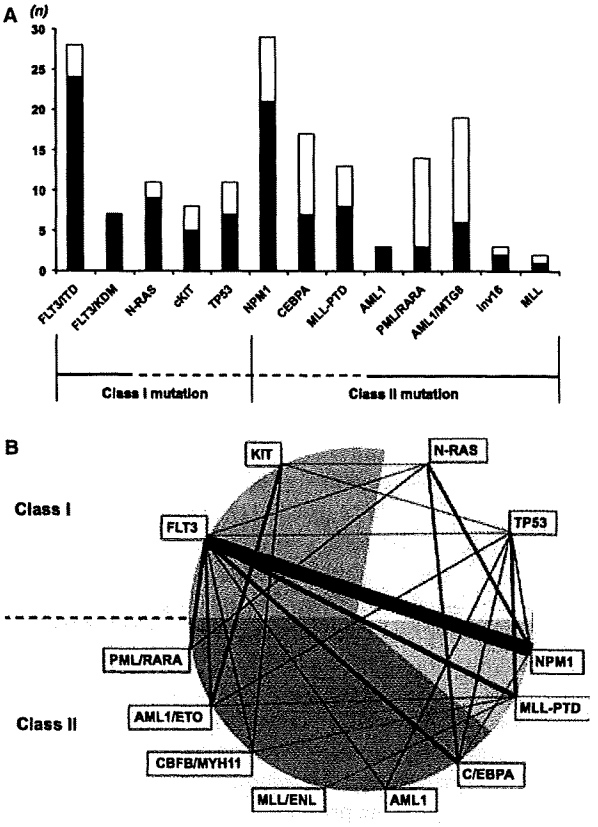

Figure 1 Prevalence and overlap pattern of class I and class II mutations in *de novo* AML. (A) We identified a total of 165 class I or class II mutations, 103 of which (62.4%) were overlapped with other mutations. Black and white bars indicate mutations with or without additional overlapped mutations, respectively. (B) Overlap pattern of each mutation. Red lines indicate mutations within the same class. Each line thickness represents the prevalence of overlap mutation. All FLT3/KDM overlapped with class II mutations, while two FLT3/ITD overlapped with class I mutations.

TP53 mutation was overlapped with a variety of gene mutations. Seven of the 11 *TP53* mutated cases showed overlap mutations: two was overlapped with *MLL*-PTD and each one with *NPM1*, *C/EBPA*, *AML1*, *cKIT*, and FLT3/ITD mutations. Cytogenetic analysis revealed that 10 *TP53* mutated cases had abnormal karyotypes: eight were complex karyotype, five of which had a deleted chromosome 17, and each one was 46XY, del(5q) and 46XY, t(8;21), del(9). Importantly, one case with *TP53* mutation and the karyotype 46XY, del(5q) harbored

Table 2 Characteristics of AML patients with overlap mutations within the same class

Age (yr)	Sex	WHO category	FAB	WBC ($\times 10^9$/L)	Mutation
Two mutations					
64	F	Not otherwise specified	M2	18.8	*cKIT, N-RAS*
46	F	Recurrent genetic abnormalities	M4	1.4	*MLL-PTD, MLL/ENL*
Three mutations					
76	M	Not otherwise specified	M4	47.5	*FLT3/ITD, TP53, MLL-PTD*
18	M	Myelodysplasia-related changes	M4	124.9	*FLT3/ITD, NPM1, C/EBPA*
50	F	Recurrent genetic abnormalities	M3	12.0	*FLT3/ITD, N-RAS, PML/RARA*
17	M	Recurrent genetic abnormalities	M2	11.0	*cKIT, TP53, AML1/ETO*
29	F	Recurrent genetic abnormalities	M4Eo	113.3	*FLT3/ITD, MLL-PTD, CBFB/MYH11*

AML, acute myeloid leukemia; WHO, World Health Organization.

FLT3/ITD, and one case with *TP53* mutation and the karyotype 46XY, t(8;21), del(9) harbored *cKIT* mutation. Although one case showed a normal karyotype, it was overlapped with the *AML1* mutation. Taken together, all *TP53* mutated cases had another genetic alterations (Fig. 2). On the other hand, a complex karyotype was found in 14 patients. Ten patients showed MLD, and eight of them had *TP53* mutation. The remaining four patients without MLD did not harbor *TP53* mutation, although three of them showed del(17) or del(17p). A genotype consisting of complex karyotype and *TP53* mutation was therefore specifically found in AML-MLD.

Prognostic implications of the mutational status

We analyzed prognostic implications of the mutational status in 130 AML patients except for acute promyelocytic leukemia. We divided AML patients into four groups: AML-MLD with or without complex karyotype and *TP53* mutation, AML with *AML1/ETO* or *CBFB/MYH11* (CBF-AML) and other type AML. Clinical characteristics of each group are shown in Table 3. Median age of the patients in CBF-AML was significantly younger than the other groups ($P = 0.012$), while there was no significant difference in median WBC count among 4 groups. The CR rate in AML-MLD with complex karyotype and *TP53* mutation (25%) was significantly lower than the other groups ($P = 0.0012$). Multivariate logistic-regression analysis revealed that WBC count (over 100×10^9/L) [odds ratio, 12.910 (95% CI: 3.101–53.742); $P = 0.0004$], wild-type *NPM1* [odds ratio, 10.640 (95% CI: 2.185–51.810); $P = 0.0034$), the genotype consisting of complex karyotype and *TP53* mutation [odds ratio, 8.755 (95% CI: 1.166–12.987); $P = 0.0271$], wild-type *C/EBPA* [odds ratio, 7.534 (95% CI: 1.111–51.103); $P = 0.0387$] and the presence of MLD [odds ratio, 3.891 (95% CI: 1.166–12.987); $P = 0.0271$] were independent unfavorable factors for achieving CR (Table 4). Furthermore, we analyzed prognostic implications of genetic alterations in addition to age, WBC count and existence of MLD. Multivariate Cox regression analysis with stepwise selection showed that the genotype consisting of complex karyotype and *TP53* mutation [odds ratio, 5.988 (95% CI: 2.681–13.333); $P < 0.0001$], not CBF-AML [odds ratio, 2.602 (95% CI: 1.107–6.116); $P = 0.0283$], FLT3/ITD [odds ratio, 1.843 (95% CI: 1.063–3.196); $P = 0.0294$] and age

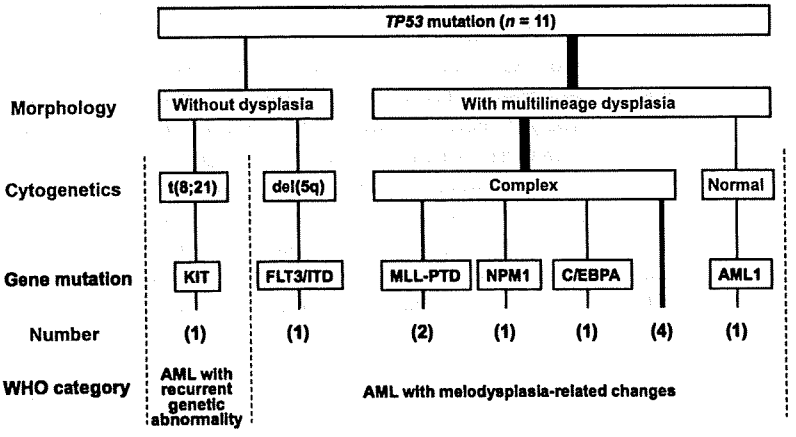

Figure 2 Association of *TP53* mutations with morphology, cytogenetics, and other mutations. *TP53* mutations were overlapped with a variety of mutations. Eight of the 11 *TP53* mutated cases showed complex karyotype, and all of them revealed morphologic MLD.

Table 3 Clinical characteristics of 130 AML patients except APL

	AML with MLD				
	With complex/ TP53 Mt.	Without complex/ TP53 Mt.	CBF-AML	Other AML	*P*-value
Number	8	26	22	74	
Age (yr)					
Median	60.5	55.5	**33.0**	53	0.012
Range	20–81	18–85	16–72	15–77	
WBC ($\times 10^9$/L)					
Median	6.6	16.9	10.3	22.9	NS
Range	1.2–22.4	0.8–139.5	3.1–113.3	0.9–351.0	
CR	**2**	19	20	60	0.0012
(%)	(25.0)	(73.1)	(90.9)	(81.1)	
Cytogenetics risk (%)					
High	8 (100)	3 (11.5)	–	10 (13.5)	
Complex	8 (100)	2 (7.7)	–	4 (5.4)	
Intermediate	–	23 (88.5)	–	64 (86.5)	
Normal	–	18 (69.2)	–	36 (48.6)	

Median age of the patients in CBF-AML was significantly younger than the other groups. The CR rate in AML-MLD with complex karyotype and *TP53* mutation was significantly lower than the other groups. Bold letters indicate significantly different groups.
AML, acute myeloid leukemia; APL, acute promyelocytic leukemia; MLD, multilineage dysplasia; CR, complete remission.

Table 4 Unfavorable risk factors for achieving CR in *de novo* AML except for APL

Factors	OR	95% CI	*P*-value
WBC count (>100 x 10^9/L)	12.910	3.101–53.742	0.0004
Wild-type *NPM1*	10.640	2.185–51.810	0.0034
Complex karyotype/TP53 mutation	8.755	1.098–69.821	0.0405
Wild-type *C/EBPA*	7.534	1.111–51.103	0.0387
Presence of MLD	3.891	1.166–12.987	0.0271

AML, acute myeloid leukemia; CR, complete remission; MLD, multilineage dysplasia.

Table 5 Unfavorable prognostic factors for overall survival in *de novo* AML except for APL

Factors	OR	95% CI	*P*-value
Complex karyotype/TP53 mutation	5.988	2.681–13.333	<0.0001
Not CBF AML	2.602	1.107–6.116	0.0283
FLT3/ITD	1.843	1.063–3.196	0.0294
Age (>60 yr)	1.764	1.086–2.865	0.0218

AML, acute myeloid leukemia.

(over 60 yr) [odds ratio, 1.764 (95% CI: 1.086–2.865); $P = 0.0218$] were poor prognostic factors for overall survival (Table 5). For disease-free survival, not CBF-AML [odds ratio, 2.475 (95% CI: 1.176–5.208); $P = 0.0169$] and *AML1* mutation [odds ratio, 8.134 (95% CI: 1.039–63.642); $P = 0.0453$] were identified to be poor prognostic factors.

Discussion

In this study, we comprehensively analyzed mutations in the *FLT3*, *cKIT*, *N-RAS*, *AML1*, *C/EBPA*, *MLL*, *NPM1*, *and TP53* genes as well as cytogenetics in 144 newly diagnosed *de novo* AML patients. We identified a total of 165 class I or class II mutations, 103 of which (62.4%) were overlapped with other analyzed mutations, supporting that multiple genetic alterations have been accumulated at the diagnosis of AML. However, overlap mutations of *PML/RARA* (3/14, 21.4%) and *AML1/ETO* (6/19, 31.6%) were infrequent. Furthermore, overlap mutations of *C/EBPA* mutations, which are frequently found in cytogenetically normal AML, were relatively infrequent (7/17, 41.2%). It is well known that *PML/RARA*, *AML1/ETO*, and *C/EBPA* mutations are associated with favorable prognosis, while recent reports revealed that additional class I mutations, such as *FLT3* and *cKIT* mutations, reduced their favorable prognosis. Our results further indicate that it is necessary to clarify whether there are unknown class I mutations overlapped with them, which influence their prognostic impacts.

We demonstrate here that most overlap mutations found in AML consisted of class I and class II mutations. Although overlap mutations within the same class were found in seven patients, five of them additionally had the other class mutation. These results suggest that most overlap mutations within the same class might be the consequence of acquiring an additional mutation after the completion both of class I and class II mutations. Therefore, it is possible that an unknown

mutation of the opposite class was acquired in two patients, whose mutations consisted of two mutations within the same class. On the other hand, it has been reported that mutations in genes functioning in different pathways can occur in the same cancer, while genes functioning in the same pathway are rarely mutated in the same sample (23). However, it was also observed that certain overlap mutational patterns violate these rules and demonstrate tissue-specific variations (23). In addition, we found that mutated genes, which overlapped with the same class mutations, were limited in *N-RAS*, *TP53*, *MLL*-PTD, and *NPM1*. As these mutations are sometimes acquired at the relapse, it is necessary to analyze whether these irregular overlap mutations cooperatively participate in the development of AML, and whether these mutations are acquired during the disease progression (18, 24).

We further demonstrate the characteristic cooperative features of *TP53* mutation in *de novo* AML. Ten of the 11 patients with *TP53* mutation showed cytogenetic abnormality, and six of them showed an additional mutation. Furthermore, additional mutations involved both class I and class II mutations. Because of the evidence that p53 mediates quiescence of normal hematopoietic stem cells, Pedersen-Bjergaard *et al.* (25) proposed that *TP53* mutation functionally represent a new class III mutation. On the other hand *TP53* has been known as a tumor suppressor gene of importance for genomic stability, and it has been suggested that leukemic progenitor accumulates additional chromosomal alterations after inactivation of *TP53* in the development of AML (26). Although it is necessary to clarify how *TP53* mutation biologically involves the accumulation of genetic alterations during the development of AML and how their interactions are associated with the leukemogenesis, the previous and our results collectively suggest that *TP53* mutation might be a distinguishable class of mutation from class I and class II mutations.

Haferlach *et al.* (27) reported that *TP53* mutations were strongly associated with the complex karyotype in AML, but the association with dysplastic morphology was not evaluated; however, our results indicate that this genotype is closely associated with dysplastic morphology regardless of the history of MDS. It has been reported that *TP53* mutation is associated with loss of chromosome band 17p13, where the *TP53* gene is located (9, 28). Deletion of 17p, which occurred by unbalanced translocation between chromosome 17p and another chromosome, monosomy 17 or i(17), is reportedly observed in 3–4% of AML and MDS and 10–15% of therapy-related MDS or AML (29–33). Furthermore, it has been reported that 17p deletion is closely associated with dysgranulopoiesis, *TP53* mutation and additional complex cytogenetic findings in AML and MDS (34, 35). In our study, deletion of 17p was identified in eight of entire 144 AML patients (5.6%), and all showed a complex karyotype. Of note is that five of eight patients with complex karyotype and *TP53* mutation showed 17p deletion, while the chromosome 17 was intact in the remaining three patients. Prognostic implication of the genotype consisting of a complex karyotype and *TP53* mutation is particularly notable as to be an independent unfavorable prognostic factor both for achieving CR and overall survival in entire *de novo* AML patients. These results collectively indicate that this genotype generates a disease entity in *de novo* AML.

Although several genetic alterations have been shown to be associated with MDS-related AML, morphologic evidence is recommended as the most available marker for the diagnosis of AML-MLD (36); however, diagnosis of dysplasia is difficult to qualify and/or quantify. Wandt *et al.* (37) demonstrated that MLD was associated with an unfavorable cytogenetic profile and that the presence of MLD was an unfavorable risk factor for achieving CR in univariate analysis but not a poor prognostic factor for either event-free or overall survival by analyzing a large number of AML patients both with and without a history of MDS. Consistently, the presence of MLD was identified to be an independent unfavorable risk factor for achieving CR by multivariate analysis, but not for long-term survival in our analysis of all AML patients. We could not identify the AML-MLD-specific genotype other than a complex karyotype and *TP53* mutation and there were some AML-MLD without any genetic alterations, indicating that AML-MLD is still genetically heterogeneous.

Acknowledgements

We would like to thank Ms. Manami Kira and Ms. Satomi Yamaji for secretarial and technical assistance. Hitoshi Kiyoi is a consultant for Kyowa-Kirin Co., Ltd. The other authors have no relevant conflicts to disclose.

References

1. Estey E, Dohner H. Acute myeloid leukaemia. *Lancet* 2006;**368**:1894–907.
2. Harris NL, Jaffe ES, Diebold J, Flandrin G, Muller-Hermelink HK, Vardiman J, Lister TA, Bloomfield CD. World Health Organization classification of neoplastic diseases of the hematopoietic and lymphoid tissues: report of the Clinical Advisory Committee meeting-Airlie House, Virginia, November 1997. *J Clin Oncol* 1999;**17**:3835–49.
3. Osumi K, Fukui T, Kiyoi H, *et al.* Rapid screening of leukemia fusion transcripts in acute leukemia by real-time PCR. *Leuk Lymphoma* 2002;**43**:2291–9.

4. Frohling S, Scholl C, Gilliland DG, Levine RL. Genetics of myeloid malignancies: pathogenetic and clinical implications. *J Clin Oncol* 2005;**23**:6285–95.
5. Mrozek K, Marcucci G, Paschka P, Whitman SP, Bloomfield CD. Clinical relevance of mutations and gene-expression changes in adult acute myeloid leukemia with normal cytogenetics: are we ready for a prognostically prioritized molecular classification? *Blood* 2007;**109**:431–48.
6. Swerdlow S, Campo E, Harris N, Jaffe E, Pileri S, Stein H, Thiele J, Vardiman J. *WHO Classification of Tumours of Haematopoietic and Lymphoid Tissues*, 4th edn. Lyon: WHO Press, 2008.
7. Speck NA, Gilliland DG. Core-binding factors in haematopoiesis and leukaemia. *Nat Rev Cancer* 2002;**2**:502–13.
8. Renneville A, Roumier C, Biggio V, Nibourel O, Boissel N, Fenaux P, Preudhomme C. Cooperating gene mutations in acute myeloid leukemia: a review of the literature. *Leukemia* 2008;**22**:915–31.
9. Fenaux P, Jonveaux P, Quiquandon I, Lai JL, Pignon JM, Loucheux-Lefebvre MH, Bauters F, Berger R, Kerckaert JP. P53 gene mutations in acute myeloid leukemia with 17p monosomy. *Blood* 1991;**78**:1652–7.
10. Slingerland JM, Minden MD, Benchimol S. Mutation of the p53 gene in human acute myelogenous leukemia. *Blood* 1991;**77**:1500–7.
11. Nakano Y, Naoe T, Kiyoi H, *et al.* Prognostic value of p53 gene mutations and the product expression in de novo acute myeloid leukemia. *Eur J Haematol* 2000;**65**:23–31.
12. Christiansen DH, Andersen MK, Pedersen-Bjergaard J. Mutations with loss of heterozygosity of p53 are common in therapy-related myelodysplasia and acute myeloid leukemia after exposure to alkylating agents and significantly associated with deletion or loss of 5q, a complex karyotype, and a poor prognosis. *J Clin Oncol* 2001;**19**:1405–13.
13. Pedersen-Bjergaard J, Christiansen DH, Desta F, Andersen MK. Alternative genetic pathways and cooperating genetic abnormalities in the pathogenesis of therapy-related myelodysplasia and acute myeloid leukemia. *Leukemia* 2006;**20**:1943–9.
14. Miyawaki S, Tanimoto M, Kobayashi T, *et al.* No beneficial effect from addition of etoposide to daunorubicin, cytarabine, and 6-mercaptopurine in individualized induction therapy of adult acute myeloid leukemia: the JALSG-AML92 study. Japan Adult Leukemia Study Group. *Int J Hematol* 1999;**70**:97–104.
15. Miyawaki S, Sakamaki H, Ohtake S, *et al.* A randomized, postremission comparison of four courses of standard-dose consolidation therapy without maintenance therapy versus three courses of standard-dose consolidation with maintenance therapy in adults with acute myeloid leukemia: the Japan Adult Leukemia Study Group AML 97 Study. *Cancer* 2005;**104**:2726–34.
16. Kiyoi H, Naoe T, Nakano Y, *et al.* Prognostic implication of FLT3 and N-RAS gene mutations in acute myeloid leukemia. *Blood* 1999;**93**:3074–80.
17. Ozeki K, Kiyoi H, Hirose Y, *et al.* Biologic and clinical significance of the FLT3 transcript level in acute myeloid leukemia. *Blood* 2004;**103**:1901–8.
18. Suzuki T, Kiyoi H, Ozeki K, *et al.* Clinical characteristics and prognostic implications of NPM1 mutations in acute myeloid leukemia. *Blood* 2005;**106**:2854–61.
19. Yamamoto Y, Kiyoi H, Nakano Y, *et al.* Activating mutation of D835 within the activation loop of FLT3 in human hematologic malignancies. *Blood* 2001;**97**:2434–9.
20. Kiyoi H, Yamaji S, Kojima S, Naoe T. JAK3 mutations occur in acute megakaryoblastic leukemia both in Down syndrome children and non-Down syndrome adults. *Leukemia* 2007;**21**:574–6.
21. Frohling S, Schlenk RF, Stolze I, Bihlmayr J, Benner A, Kreitmeier S, Tobis K, Dohner H, Dohner K. CEBPA mutations in younger adults with acute myeloid leukemia and normal cytogenetics: prognostic relevance and analysis of cooperating mutations. *J Clin Oncol* 2004;**22**:624–33.
22. Paschka P, Marcucci G, Ruppert AS, *et al.* Adverse prognostic significance of KIT mutations in adult acute myeloid leukemia with inv(16) and t(8;21): a Cancer and Leukemia Group B Study. *J Clin Oncol* 2006;**24**:3904–11.
23. Yeang CH, McCormick F, Levine A. Combinatorial patterns of somatic gene mutations in cancer. *FASEB J* 2008;**22**:2605–22.
24. Nakano Y, Kiyoi H, Miyawaki S, Asou N, Ohno R, Saito H, Naoe T. Molecular evolution of acute myeloid leukaemia in relapse: unstable N-ras and FLT3 genes compared with p53 gene. *Br J Haematol* 1999;**104**:659–64.
25. Pedersen-Bjergaard J, Andersen MK, Andersen MT, Christiansen DH. Genetics of therapy-related myelodysplasia and acute myeloid leukemia. *Leukemia* 2008;**22**:240–8.
26. Castro PD, Liang JC, Nagarajan L. Deletions of chromosome 5q13.3 and 17p loci cooperate in myeloid neoplasms. *Blood* 2000;**95**:2138–43.
27. Haferlach C, Dicker F, Herholz H, Schnittger S, Kern W, Haferlach T. Mutations of the TP53 gene in acute myeloid leukemia are strongly associated with a complex aberrant karyotype. *Leukemia* 2008;**22**:1539–41.
28. Jonveaux P, Fenaux P, Quiquandon I, Pignon JM, Lai JL, Loucheux-Lefebvre MH, Goossens M, Bauters F, Berger R. Mutations in the p53 gene in myelodysplastic syndromes. *Oncogene* 1991;**6**:2243–7.
29. Fenaux P, Morel P, Lai JL. Cytogenetics of myelodysplastic syndromes. *Semin Hematol* 1996;**33**:127–38.
30. Le Beau MM, Albain KS, Larson RA, Vardiman JW, Davis EM, Blough RR, Golomb HM, Rowley JD. Clinical and cytogenetic correlations in 63 patients with therapy-related myelodysplastic syndromes and acute nonlymphocytic leukemia: further evidence for characteristic abnormalities of chromosomes no. 5 and 7. *J Clin Oncol* 1986;**4**:325–45.
31. Pedersen-Bjergaard J, Philip P. Balanced translocations involving chromosome bands 11q23 and 21q22 are highly characteristic of myelodysplasia and leukemia following

therapy with cytostatic agents targeting at DNA-topoisomerase II. *Blood* 1991;**78**:1147–8.
32. Soenen V, Preudhomme C, Roumier C, Daudignon A, Lai JL, Fenaux P. 17p Deletion in acute myeloid leukemia and myelodysplastic syndrome. Analysis of breakpoints and deleted segments by fluorescence in situ. *Blood* 1998;**91**:1008–15.
33. Merlat A, Lai JL, Sterkers Y, Demory JL, Bauters F, Preudhomme C, Fenaux P. Therapy-related myelodysplastic syndrome and acute myeloid leukemia with 17p deletion. A report on 25 cases. *Leukemia* 1999;**13**:250–7.
34. Sessarego M, Ajmar F. Correlation between acquired pseudo-Pelger-Huet anomaly and involvement of chromosome 17 in chronic myeloid leukemia. *Cancer Genet Cytogenet* 1987;**25**:265–70.
35. Ahuja H, Bar-Eli M, Arlin Z, Advani S, Allen SL, Goldman J, Snyder D, Foti A, Cline M. The spectrum of molecular alterations in the evolution of chronic myelocytic leukemia. *J Clin Invest* 1991;**87**:2042–7.
36. Vardiman JW, Harris NL, Brunning RD. The World Health Organization (WHO) classification of the myeloid neoplasms. *Blood* 2002;**100**:2292–302.
37. Wandt H, Schakel U, Kroschinsky F, Prange-Krex G, Mohr B, Thiede C, Pascheberg U, Soucek S, Schaich M, Ehninger G. MLD according to the WHO classification in AML has no correlation with age and no independent prognostic relevance as analyzed in 1766 patients. *Blood* 2008;**111**:1855–61.

Int J Hematol (2009) 90:37–43
DOI 10.1007/s12185-009-0337-y

ORIGINAL ARTICLE

High-resolution melting analysis for a reliable and two-step scanning of mutations in the tyrosine kinase domain of the chimerical *bcr-abl* gene

Yuko Doi · Daisuke Sasaki · Chiharu Terada · Sayaka Mori · Kazuto Tsuruda · Emi Matsuo · Yasushi Miyazaki · Kazuhiro Nagai · Hiroo Hasegawa · Katsunori Yanagihara · Yasuaki Yamada · Shimeru Kamihira

Received: 12 March 2009 / Revised: 7 April 2009 / Accepted: 22 April 2009 / Published online: 23 May 2009

Abstract For relevant imatinib therapy against Philadelphia (Ph)-positive leukemias, it is essential to monitor mutations in the chimerical *bcr-abl* tyrosine kinase domain (TKD). However, there is no universally acceptable consensus on how to efficiently identify mutations in the target TKD. Recently, high-resolution melting (HRM) technology was developed, which allows gene scanning using an inexpensive generic heteroduplex-detecting dsDNA-binding dye. This study aimed to validate the introduction of HRM in a practical clinical setting for screening of mutations in sporadic sites of the chimerical *bcr-abl* TKD. All chimerical and wild-type *abl* TKD regions selectively amplified were used for HRM assays and direct sequencing. The HRM test had approximately 5–90% detection sensitivity for mutations. In contrast to mixture samples with mutant and wild-type cells, all mutant cell samples had indeterminate melting curves equivalent to those of the wild-type due to formation of only a homodulex. This issue was improved by the addition of exogenous wild-type DNA after PCR. Subsequently, HRM results gave a high accordance rate of 97.8% (44/45 samples) compared to the sequencing data. The discordant results in one appear to be due to unsuccessful amplification. Thus, HRM may be considered to be suitable for reliable scanning of mutations in the chimerical *abl* TKD in a clinical setting.

Keywords Ph · *bcr-abl* · Mutation · Melting analysis · HRM

Y. Doi · D. Sasaki · C. Terada · S. Mori · K. Tsuruda · K. Nagai · H. Hasegawa · K. Yanagihara · Y. Yamada · S. Kamihira (✉)
Department of Laboratory Medicine,
Nagasaki University Graduate School
of Biomedical Sciences, 1-7-1 Sakamoto,
Nagasaki 852-8501, Japan
e-mail: kamihira@nagasaki-u.ac.jp

E. Matsuo · Y. Miyazaki
Department of Hematology,
Nagasaki University Graduate School
of Biomedical Sciences, 1-7-1 Sakamoto,
Nagasaki 852-8501, Japan

1 Introduction

The chemical agent, imatinib, has a high therapeutic response for diseases carrying the chimerical *bcr-abl* gene. For example, the first imatinib treatment was reported to give approximately 80 and 60% complete molecular response rates in chronic myelogenous leukemia (CML) and Philadelphia (Ph)-positive acute lymphoblastic leukemia (ALL), respectively [1, 2]. However, in many cases, mutations in the chimerical *abl* tyrosine kinase domain (TKD) were revealed to precede resistance to imatinib, resulting in disease relapse and progression to advanced disease. At present, although it is known that there are several causative factors in resistance, such as expression of a rapid drug efflux protein and non-*bcr-abl*-dependent transformation involving the *src* family, TKD mutations in the chimerical gene are thought to play a major role in resistance acquisition [3]. Therefore, detection of mutations becomes essential in cases treated with imatinib. Moreover, mutations associated with imatinib therapy emerge as a Ph-positive subclone from minimal residual leukemia (MRD) even in the hematological remission period [4, 5]. This indicates the need for highly sensitive tests to detect only Ph-positive leukemic clones. To date, several methods to analyze mutations including direct and subcloning sequencing have been employed, but the respective methods have merits and demerits and are not

always sensitive [6]. Recently, to analyze genetic variations (SNPs, mutations and methylations), a novel melting analysis called high-resolution melting (HRM) with an automated instrument and real-time PCR apparatus was used [7, 8]. HRM is used to characterize samples according to their dissociation profile as they transit from double-strand DNA (dsDNA) to single-strand (ssDNA). Therefore, mixture samples with mutant and wild-type cells are easily identified by differences in melting curve shapes. Mutant sequence variants produce a Tm shift compared with the wild-type [9]. In addition, it is a reliable- and closed-tube system without high-cost fluorescence probes [10, 11]. Thus, to introduce HRM assays in clinical settings to detect Ph-positive subclones with *bcr-abl* kinase domain mutations, the relevance and validation of the assay prior to direct sequencing was studied.

2 Materials and methods

2.1 Samples and processing of cDNA

A total of 19 Ph-positive samples were used, consisting of 10 unlinked and already mutation-known specimens, 8 fresh practical samples from 6 patients with CML, 2 patients with ALL and one sample from a Ph-positive K562 cell line. All patients with Ph-positive leukemias were being treated with imatinib at 400–800 mg per day and had hematological remission, but were positive for *bcr-abl* real-time RT PCR. As controls, 16 peripheral blood samples from normal volunteers and 10 cell lines consisting of HTLV-1-associated cell lines (Hut102, KK1, KOB, OMT, MT2, SO4, ST1), T cell lines of Jurkat and MOLT4, and the monocytic line U937 were used.

Total RNA was extracted from total leukocyte guanidinium thiocyanate lysates using ISOGEN (Nippon gene, Toyama, Japan). cDNA was synthesized using oligo-dT primers and Superscript III reverse transcriptase (Invitrogen, Carsland, CA, USA). Practical and stocked samples used in this study were applied under the approval (15040708) of the ethics committee and the condition of the criteria of the Japanese Association of Laboratory Medicine.

2.2 Study design for HRM assay in the chimerical *abl* TKD region

Our study for the detection of mutation was designed in a two-step manner: firstly, genetic alteration screening by HRM analysis (Fig. 1), using the LightCycler 480 (Roche Molecular System, Alameda, CA, USA) for HRM and real-time thermal cycling; secondly, only samples positively screened by HRM were directly sequenced. First of all, each sample was examined for *bcr-abl* chimerical status by

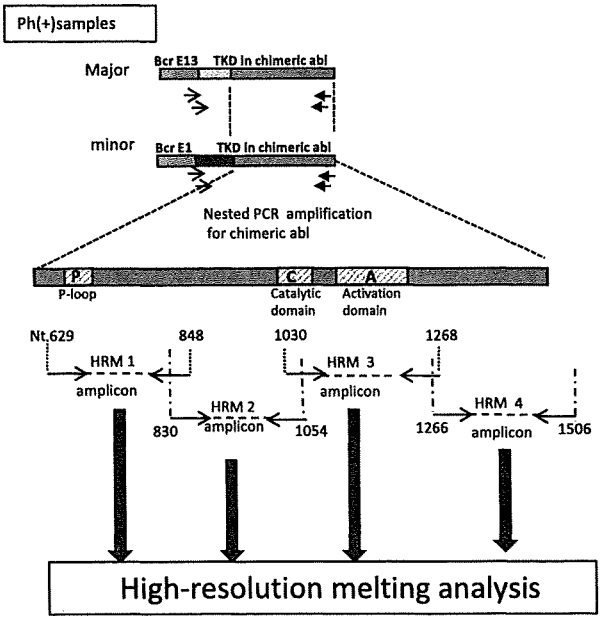

Fig. 1 Study design of high-resolution melting (HRM) and the structure of the tyrosine kinase domain (TKD). Firstly, a part of chimerical *bcr-abl* TKD is selectively amplified by nested PCR. Using amplified chimerical *bcr-abl* products as a template, the second PCR for the HRM assay is performed, generating four intercalating dye amplicons, HRM-1, -2, -3 and -4. Then, HRM analyses were done by using the LightCycler Gene Scanning Application

the conventional method [12]. If positive for major or minor chimerical types, these *bcr-abl* kinase domains were selectively amplified, generating a fragment of 1504 bp for b2/a2 and 1579 bp for b3/a2, using primers previously reported [13].

For HRM analysis, PCR products of 50–250 bp length are recommended for best discrimination. Therefore, we applied a modified method previously reported by Poláková et al. [10], generating 4 amplicons, designated as HRM1, 2, 3 and 4 of 220, 225, 239 and 241 bp, corresponding to nt 629–848, 830–1054, 1030–1268, and 1266–1506 (NM_005157), respectively. For HRM, a PCR reaction was performed in 20 µl reaction volumes containing 1 µl of 1/200 diluted template generated as described above, Master Mix, Taq DNA polymerase, dNTP mix, HRM dye, 3 mM $MgCl_2$, primers [10], and 1 M GC melt, according to the instructions of Roche Applied Science (Manheim, Germany). The PCR was monitored by real-time cycling and a strong fluorescent signal was generated only when bound to dsDNA, that is the touchdown PCR cycling and HRM conditions [14]. HRM melting curve data were obtained by slowly increasing the temperature, from 60 to 90°C at a rate of 100 acquisitions per 1°C. The melting status and changes in Tm value were analyzed using the Roche HRM algorithm (Gene Scanning Software, Roche Supplied Science, Manheim, Germany),